

## Avoided Critical Behavior in Dynamically Forced Wetting

Jacco H. Snoeijer,<sup>1</sup> Giles Delon,<sup>1</sup> Marc Fermigier,<sup>1</sup> and Bruno Andreotti<sup>1</sup>

<sup>1</sup>*Physique et Mécanique des Milieux Hétérogènes, UMR 7636 CNRS-ESPCI, 10 rue Vauquelin, 75231 Paris Cedex 05, France*  
(Received 3 November 2005; published 5 May 2006)

A solid object can be coated by a nonwetting liquid since a receding contact line cannot exceed a critical speed. In this Letter we study the dynamical wetting transition at which a liquid film gets deposited by withdrawing a vertical plate out of a liquid reservoir. It has recently been predicted that this wetting transition is critical with diverging time scales and coincides with the disappearance of stationary menisci. We demonstrate experimentally and theoretically that the transition is due to the formation of a solitary wave, well below the critical point. As a consequence, relaxation times remain finite at threshold. The structure of the liquid deposited on the plate involves a capillary ridge that does not trivially match the Landau-Levich film.

DOI: 10.1103/PhysRevLett.96.174504

PACS numbers: 47.10.-g, 68.08.Bc

Wetting and dewetting phenomena are encountered in a variety of environmental and technological contexts, ranging from the treatment of plants to oil recovery and coating. Yet, their dynamics can not be captured within the framework of classical hydrodynamics—with the usual no-slip boundary condition on the substrate—since the viscous stress diverges at the contact line [1,2]. The description of moving contact lines has remained a great challenge, especially because it involves a wide range of length scales. In between molecular and millimetric scales, the strong viscous stresses are balanced by capillary forces. In this zone, the slope of the free surface varies logarithmically with the distance to the contact line so that the interface is strongly curved, even down to small scales [3,4]. Ultimately, the intermolecular forces due to the substrate introduce the physical mechanism that cuts off this singular tendency [3–5]. The problem remains highly controversial, however, as none of the existing experiments has been able to discriminate between the various proposed regularizations.

The motion of *receding* contact lines is limited by a maximum speed beyond which the interface gives way to liquid deposition. Drops sliding down a window develop singular cusplike tails that, at high velocities, emit little drops [6]. Similarly, solid objects can be coated by a nonwetting liquid when withdrawn fast enough from a liquid bath [7–9]. The relevant dimensionless parameter for these experiments is the capillary number  $Ca = \eta U / \gamma$ , which represents the velocity  $U$ , rescaled by viscosity  $\eta$  and surface tension  $\gamma$ . Recently, this wetting transition to liquid deposition has been interpreted in a full-scale hydrodynamic model, as a matching problem between the boundary conditions imposed at both ends of the scale range: the highly curved contact line zone and the macroscopic flow [10,11]. Above a critical  $Ca_c$ , stationary solutions cease to exist. It has furthermore been argued, as is generic for saddle-node bifurcations, that relaxation times should diverge at this critical point [12,13].

In this Letter we unravel the nature of the dynamical wetting transition in the classical setup of a dip-coating

experiment, in which a plate is withdrawn vertically from a liquid bath. We demonstrate that the transition occurs *before* the predicted critical point, due to the appearance of a solitary wave that has the structure of a ridge (Fig. 1). This ridge is very different from the rim observed in dewetting of thin films [14], both in structure as well as in its physical origin. This provides a novel perspective on wetting dynamics, in particular, since we show that the ridge serves as a sensitive probe for the nanoscale physics at the contact line.

*Experimental setup.*—We study the dynamics at the forced wetting transition by withdrawing a vertical plate from a bath of nonwetting liquid. The experiments were performed using a 50 mm  $\times$  100 mm silicon wafer coated with a fluorinated surfactant FC725 (sold by 3M), which is withdrawn vertically from a bath of silicone oil (viscosity  $\eta = 4.95$  Pa s, surface tension  $\gamma = 0.0203$  N m<sup>-1</sup>, density  $\rho = 970$  kg m<sup>-3</sup>, molecular size 70 nm). The silicone oil is partially wetting the plate, with a static contact angle  $\theta_s = 51.5^\circ$  for a receding contact line ( $57^\circ$  for an advancing one). The plate velocity  $U_p$  is controlled within a

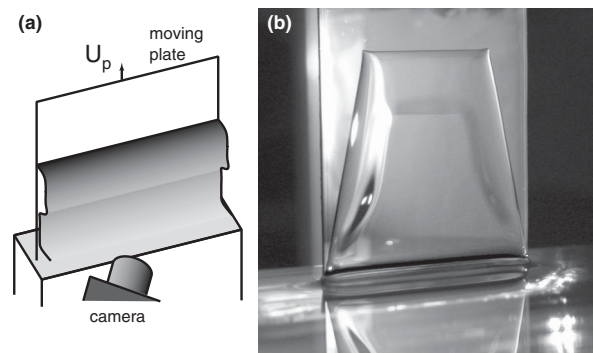


FIG. 1. (a) Schematic representation of the experiment: a vertical plate is withdrawn from a liquid bath at constant velocity  $U_p$ . Above the transition, a capillary ridge starts propagating upwards. (b) Photograph of the experiment. The inclined contact lines are induced by the edges of the plate. This Letter focuses on the horizontal central zone.

micron per second by a stepper motor. In the remainder the capillary number is based upon the *plate velocity*,  $Ca = \eta U_p / \gamma$ . Above the transition we have reconstructed the shape of the entrained film by placing a thin wire parallel to the plate, a few millimeters from the liquid film. The mirror image of the wire (reflected in the silicon plate) is distorted by refraction through the liquid-vapor interface. The displacement of the image of the wire gives the local interface slope from which we reconstruct the capillary ridge, by integration.

*Experimental results.*—We first consider plate velocities below the wetting transition. After the plate is set into motion one finds that the contact line evolves towards an equilibrium height  $z_{cl}$  above the liquid reservoir (Fig. 2). The relaxation of the meniscus toward  $z_{cl}$  is exponential with a well-defined time scale. The entrainment transition is defined by the plate velocity beyond which the contact line no longer equilibrates, but continues propagating upwards. It has been predicted that the transition is due to a critical point that is characterized by diverging time scales at threshold [12,13]. Figure 2 clearly shows, however, that the relaxation time remains finite in the experiment [15], even right at the transition ( $Ca^* = 9.1 \times 10^{-3} \pm 2 \times 10^{-4}$ ). This is a first strong indication that entrainment already occurs *before* the critical point at which stationary solutions disappear.

We unravel the mechanism that is responsible for this avoided critical behavior by following the interface profile during entrainment. Surprisingly, the dynamics above the transition does not immediately give rise to a flat “Landau-Levich” film [16], but involves an intermediate ridgelike structure that propagates upwards (Fig. 1). The evolution of the free surface as a function of time is shown in Fig. 3. One first observes the formation of a ridge, right behind the contact line, which after a short transient stage evolves towards a flat zone of constant thickness  $h_r$ . This plateau stretches in the course of the experiment. The contact line

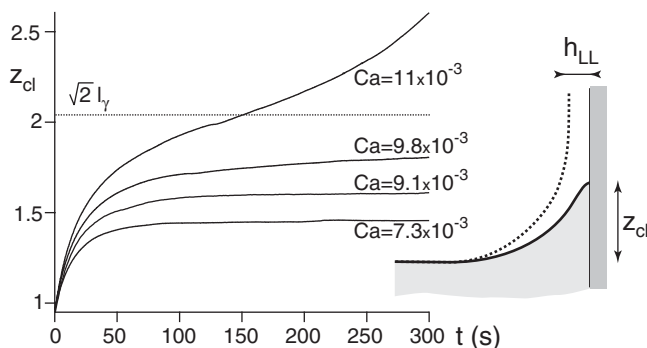


FIG. 2. Evolution of the contact line. Right: Below the entrainment threshold, the contact line equilibrates at a height  $z_{cl}$ . Above the transition, the liquid bath matches to the Landau-Levich film of thickness  $h_{LL}$ . Left: Even right at the transition, the contact line still relaxes exponentially towards  $z_{cl}$  with a finite relaxation time.

moves upwards at a constant velocity  $U_{cl}$ . This front of the entrained liquid does not directly match onto the Landau-Levich film but involves a sharp capillary jump. This jump propagates upwards with a well-defined velocity  $U_j$ , which is lower than  $U_{cl}$ , while the shape of the shock remains unaltered. The Landau-Levich film that matches to the bath only appears behind this capillary shock (the bath is not shown in the figure). Note that very similar structures play a crucial role for the stability of advancing contact lines, driven by Marangoni forces [17].

The photograph of Fig. 1(b) reveals that there is no liquid entrainment at the edges of the plate. This gives rise to inclined contact lines at the sides that have a lower upwards velocity. As a consequence, the sharp corners intersecting the horizontal contact line move inward and ultimately meet to form a single corner [7]. Similar corner structures have been observed at the rear of sliding drops [6]. In the remainder we focus on the horizontal zone in the middle of the plate.

*Theory for the ridge.*—The remarkable structure of the liquid interface can be understood in terms of a matching among 3 zones: (i) the contact line leaving a flat film, (ii) the Landau-Levich film connected to the bath, (iii) the capillary jump matching the two flat zones. This is illustrated in Fig. 4, showing a piecewise reconstruction of the free surface. We show below that the thickness of the ridge,  $h_r$ , is solely determined by the physics at the contact line and that, in general, this does not match the Landau-Levich thickness  $h_{LL}$ . The emergence of a capillary shock matching the two film solutions is then a generic feature of free surface flows. The conditions under which these shocks occur have been discussed in detail for contact lines driven by Marangoni forces [17,18] and countercurrent two-phase flows [19].

Since each of these structures propagate with a well-defined velocity, we consider profiles  $h(z - ct)$ . These profiles are computed numerically (using a semi-implicit algorithm), within the framework of lubrication theory,

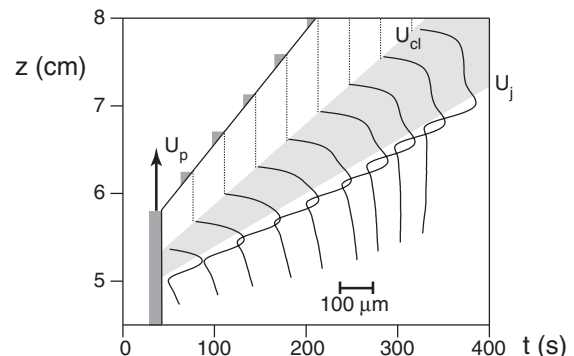


FIG. 3. Temporal evolution of the free surface at  $Ca = 32 \times 10^{-3}$ , determined by placing a thin wire in front of the plate. The contact line propagates upwards at a velocity  $U_{cl}$  larger than that of the capillary jump  $U_j$ . Note that the jump maintains a constant shape throughout the experiment.

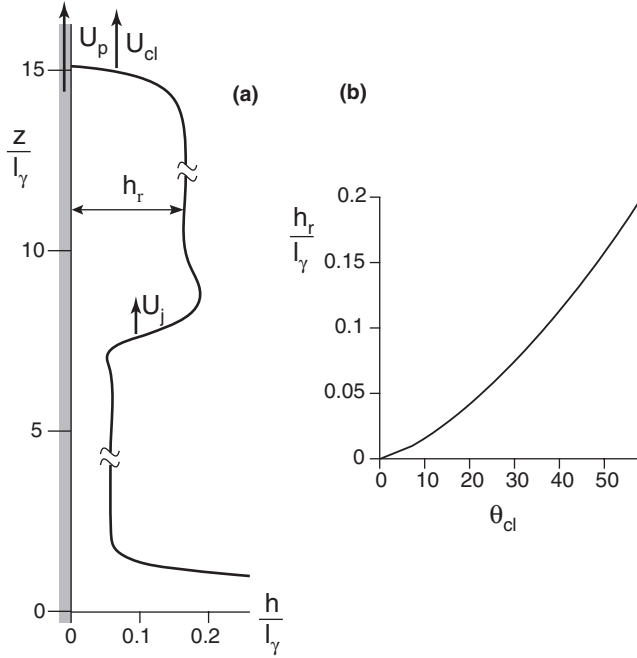


FIG. 4. (a) Cross section of the interface computed numerically from Eqs. (1) and (2), at  $Ca = 17 \times 10^{-3}$ ; we have shown that  $h_r$  does not depend on  $Ca$ . (b)  $h_r$  versus microscopic contact angle  $\theta_{cl}$ . To reproduce the experimental  $h_r = 0.165l_\gamma$  using the static angle  $\theta_s = 51.5^\circ$ , we fixed  $l_s/l_\gamma = 1.3 \times 10^{-5}$  (see text).

which is the standard tool for free surface flows [20]:

$$\partial_t h + \partial_z(hU) = 0, \quad (1)$$

$$\gamma \partial_z \kappa - \rho g + \frac{3\eta(U_p - U)}{h(h + 3l_s)} = 0. \quad (2)$$

$\kappa$  denotes the curvature of the interface, while  $U(z, t)$  is the (depth-averaged) fluid velocity inside the film. The first equation is mass conservation, while the second represents the force balance between surface tension  $\gamma$ , gravity  $\rho g$ , and viscosity  $\eta$ , respectively—in the experiments the Reynolds number is typically  $Re = 10^{-10}$ , so that inertial effects are negligible. For simplicity we have chosen to resolve the viscous singularity at the contact line using a standard Navier slip condition with microscopic slip length  $l_s$  [21–23].

Dimensional analysis of Eq. (2) reveals that the capillary length  $l_\gamma = \sqrt{\gamma/\rho g}$  is the relevant length scale of the problem. The relevant velocity scale is  $\gamma/\eta$ , which also appears in the capillary number  $Ca = \eta U_p/\gamma$ .

From Eq. (2) it clear that a flat film (curvature  $\kappa = 0$ ) can in principle exist for arbitrary thickness

$$h_{\text{film}} = l_\gamma \sqrt{3(U_p - U)\eta/\gamma}. \quad (3)$$

The fluid velocity inside the film adjusts itself such that the upwards viscous drag balances the weight of the film. A thickness gets selected only once an additional condition is

imposed. Landau and Levich [16] studied the problem of an infinite flat film that is entrained along the plate out of liquid reservoir. In this case, the matching to the bath results into the scaling  $h_{LL} \propto l_\gamma Ca^{2/3}$ .

Similarly, the additional condition of a contact line, now at the upper end of the film, provides a selection of the ridge height  $h_r$ . This can be seen by following the solutions with initial conditions close to the flat film,  $h(z) = h_r(1 - \epsilon e^{-sz})$ , toward the contact line: each  $h_r$  will yield a single value for the microscopic contact angle  $\theta_{cl}$ . Or vice versa, the height of the ridge is uniquely determined by this angle, i.e.,  $h_r(\theta_{cl})$ . This dependence has been plotted in Fig. 4(b), for a fixed value of  $l_s$ .

We emphasize that the height of the ridge and of the Landau-Levich film are determined by independent physical mechanisms, so that in general  $h_r \neq h_{LL}$ . Close to the transition we always find that  $h_r > h_{LL}$ . The matching between these films involves an intermediate structure, which we write as  $h(z - U_j t)$ . From mass conservation between the two films, one derives [18]

$$\frac{\eta}{\gamma} U_j = Ca - \frac{h_r^2 + h_r h_{LL} + h_{LL}^2}{3l_\gamma^2}, \quad (4)$$

which nicely fits the experimental data for the jump velocity  $U_j$  (Fig. 5). Here,  $h_{LL}$  has been taken according to the Landau-Levich scaling, while  $h_r$  has been calibrated from the experiment (see below).

*The threshold velocity for entrainment.*—We now show that the threshold of entrainment is not determined by the critical point at which stationary meniscus solutions disappear, but by the observed ridge structure. To do so, we

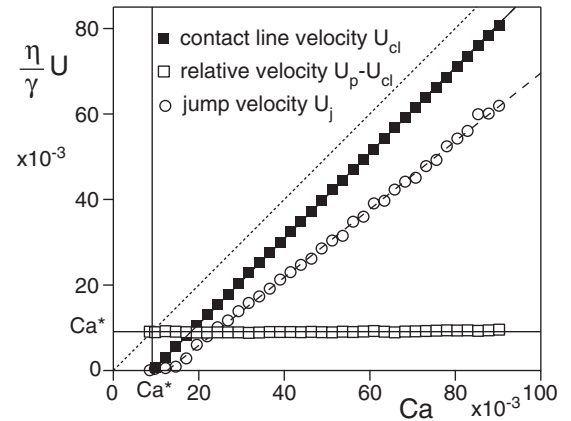


FIG. 5. Rescaled velocities of the contact line  $U_{cl}$  and the capillary jump  $U_j$ , and relative velocity  $U_p - U_{cl}$ , as a function of  $Ca$  based on the plate velocity. The entrained contact line maintains a constant velocity with respect to the plate. This velocity coincides with the entrainment threshold (solid line), indicating that the entrainment transition is due to the appearance of the ridge rather than to the disappearance of the static meniscus solution. The velocity of the jump with respect to the plate is well predicted by Eq. (4) (dashed line).

measured the velocities  $U_{cl}$ ,  $U_j$  in the reference frame of the liquid reservoir (Fig. 5). The crucial quantity is the *relative* velocity between the plate and the entrained contact line, which rescaled by  $\gamma/\eta$  simply reads

$$\text{Ca}^* = (U_p - U_{cl}) \frac{\eta}{\gamma} = \frac{1}{3} (h_r/l_\gamma)^2. \quad (5)$$

The relation with  $h_r$  follows from Eq. (3). As we have seen that  $h_r$  is solely determined by  $\theta_{cl}$ , the relative velocity  $\text{Ca}^*$  should be completely independent of  $\text{Ca}$ . This is confirmed by Fig. 5: upon increasing the plate velocity, the contact line will move faster in the lab frame in order to maintain a constant velocity difference with respect to the plate. The observed value  $\text{Ca}^* = 9.1 \times 10^{-3}$  implies  $h_r = 0.165l_\gamma$ . As Eq. (5) for flat films can be obtained directly from the Navier-Stokes equations, this result does not depend on any hypothesis for the contact line.

We find experimentally that the threshold for entrainment precisely coincides with  $\text{Ca}^*$  (Fig. 5). This observation is in striking contrast with theoretical predictions that the transition occurs at a critical  $\text{Ca}_c$ , at which the stationary meniscus solutions disappear. We numerically find from Eq. (2) that the ridge velocity  $\text{Ca}^*$  is typically 15% smaller than this critical  $\text{Ca}_c$  (see also Ref. [24]). Hence, the transition is *precritical* in the sense that the critical point is avoided through the moving ridge solution. The dynamics of the film is such that this solution nucleates as soon as it is possible, i.e., for  $U_{cl} = 0$ . This explains the observation of Fig. 2, which showed that relaxation times remain finite even right at the transition.

*Discussion.*—We have shown that for nonwetting liquids, the deposition of a Landau-Levich film involves a remarkable ridgelike structure. This ridge emerges due to a mismatching between the liquid reservoir and the contact line zone at the front of the film. Secondly, we have shown that the threshold velocity for the entrainment transition is determined by the ridge velocity  $\text{Ca}^*$ , and not by the bifurcation at which stationary menisci solutions disappear [25]. Therefore, the transition is characterized by finite relaxation times, and the critical point is avoided. This appears to be in contrast with measurements by Sedev and Petrov [9], on the dewetting of fibers of radii well below the capillary length. They claim that the transition occurs when the interface, at large scale, takes the critical shape corresponding to a perfectly wetting liquid. This difference may be due to the curvature of the fibers, which introduce a new parameter: when the radius of the fiber becomes comparable to  $l_\gamma$ , the relative values of  $\text{Ca}^*$  and  $\text{Ca}_c$  will change. Our preliminary experiments on forced wetting of thin fibers reveal that the ridge structure *does* persist around the transition.

Another interesting perspective is that the ridge properties originate directly from the physics at the contact line,

in particular, from the slip length  $l_s$  and the microscopic contact angle. Whether or not one should recover the *static* angle  $\theta_s$  at this ultimate scale is hotly debated. While in the presented lubrication model one requires a reasonable value for the slip length (about 20 nm) to reproduce the experimental ridge velocity from a slope  $\theta_s$ , this obviously remains an important open problem.

We thank J. Bico, J. Eggers, and L. Limat for fruitful discussions and P. Jenffer for technical assistance. J. H. S. acknowledges financial support by a Marie Curie Action FP6 (MEIF-CT2003-502006).

- 
- [1] C. Huh and L. E. Scriven, *J. Colloid Interface Sci.* **37**, 196 (1971).
  - [2] E. B. Dussan, V. Davis, and S. H. Davis, *J. Fluid Mech.* **65**, 71 (1974).
  - [3] O. V. Voinov, *Fluid Dyn.* **11**, 714 (1976).
  - [4] R. G. Cox, *J. Fluid Mech.* **168**, 169 (1986).
  - [5] L. M. Pismen and Y. Pomeau, *Phys. Rev. E* **62**, 2480 (2000).
  - [6] T. Podgorski, J.-M. Flesselles, and L. Limat, *Phys. Rev. Lett.* **87**, 036102 (2001).
  - [7] T. D. Blake and K. J. Ruschak, *Nature (London)* **282**, 489 (1979).
  - [8] D. Quéré, *C.R. Acad. Sci., Ser. II* **313**, 313 (1991).
  - [9] R. V. Sedev and J. G. Petrov, *Colloids Surf.* **53**, 147 (1991).
  - [10] J. Eggers, *Phys. Rev. Lett.* **93**, 094502 (2004).
  - [11] J. Eggers, *Phys. Fluids* **17**, 082106 (2005).
  - [12] R. Golestanian and E. Raphael, *Europhys. Lett.* **55**, 228 (2001).
  - [13] R. Golestanian and E. Raphael, *Phys. Rev. E* **64**, 031601 (2001).
  - [14] C. Redon, F. Brochard-Wyart, and F. Rondelez, *Phys. Rev. Lett.* **66**, 715 (1991).
  - [15] More detailed measurements will be presented elsewhere.
  - [16] L. D. Landau and B. V. Levich, *Acta Physicochimica URSS* **17**, 42 (1942).
  - [17] A. L. Bertozzi, A. Münch, X. Fanton, and A. M. Cazabat, *Phys. Rev. Lett.* **81**, 5169 (1998).
  - [18] A. L. Bertozzi, A. Münch, and M. Shearer, *Physica (Amsterdam)* **134D**, 431 (1999).
  - [19] T. M. Segin, B. S. Tilly, and L. Kondic, *J. Fluid Mech.* **532**, 217 (2005).
  - [20] A. Oron, S. H. Davis, and S. G. Bankoff, *Rev. Mod. Phys.* **69**, 931 (1997).
  - [21] E. Lauga and H. A. Stone, *J. Fluid Mech.* **489**, 55 (2003).
  - [22] R. Pit, H. Hervet, and L. Léger, *Phys. Rev. Lett.* **85**, 980 (2000).
  - [23] C. Cottin-Bizonne, B. Cross, A. Steinberger, and E. Charlaix, *Phys. Rev. Lett.* **94**, 056102 (2005).
  - [24] L. M. Hocking, *Eur. J. Appl. Math.* **12**, 195 (2001).
  - [25] We have tried to approach the critical point by quasistatically increasing the plate velocity. The entrainment transition always occurred at the same velocity  $\text{Ca}^*$ , well below the critical point.